

# FAST SODIUM CURRENT IN CARDIAC MUSCLE

## A QUANTITATIVE DESCRIPTION

LISA EBIHARA AND EDWARD A. JOHNSON, *Department of Physiology, Duke University Medical Center, Durham, North Carolina 27710 U.S.A.*

**ABSTRACT** The voltage and time-dependence of the tetrodotoxin sensitive, fast sodium current in cardiac muscle is described with the Hodgkin-Huxley formalism using two-microelectrode, voltage-clamp data obtained by Ebihara et al. (1980, *J. Gen. Physiol.*, 75:437) from small spherical clusters of tissue-cultured 11-d-old embryonic heart cells. The data chosen from that study for quantitative analysis was obtained at 37°C and in standard tissue-culture medium; it was not smoothed, and the capacitive transient was sufficiently brief to make its removal unnecessary. The sodium current,  $I_{Na}$ , is considered to be given by the following equation:  $I_{Na} = \bar{g}_{Na} m^3 h (V - V_{Na})$ , where  $\bar{g}_{Na}$  is a constant (23 mS),  $V_{Na}$  is the sodium equilibrium potential (29 mV), and  $m$  and  $h$  are independent, first order, dimensionless variables, which can vary between 0 and 1, as defined by the following differential equations.  $dm/dt = \alpha_m(1 - m) - \beta_m m$  and  $dh/dt = \alpha_h(1 - h) - \beta_h h$ , where the rate coefficients,  $\alpha_m = [0.32 \times (V + 47.13)]/[1 - \exp(V + 47.13)]$  and  $\beta_m = 0.08 \times \exp(-V/11)$ . For potentials more positive than -40 mV,  $\alpha_h = 0$  and  $\beta_h = 1/0.13 \{ \exp[(V + 10.66)/-11.1] + 1 \}$ , and for potentials more negative than -40 mV,  $\alpha_h = 0.135 \times \exp[(-80 - V)/6.8]$  and  $\beta_h = 3.56 \times \exp(0.079V) + 3.1 \times 10^5 \exp(0.35V)$ . These functions of potential are similar to those of the squid at 15°C, except that their magnitudes are larger (faster). Using these model equations the membrane current in a membrane patch with and without a series resistance was simulated. For the value of series resistance estimated for the preparation from which the analyzed data were obtained, the effects of series resistance on the shape and magnitude of the inward transient current were found to be minimal. It was concluded that there should be no large errors in the data, even in the absence of complete series resistance compensation.

## INTRODUCTION

Voltage-clamp studies of the ionic currents in cardiac muscle have been greatly hampered by the complex morphology of most naturally occurring preparations of cardiac muscle and by limitations in available voltage-clamp techniques (Johnson and Lieberman, 1971; Reuter, 1979). This is especially true for the early fast sodium current. There is no detailed information about its kinetic behavior under physiological conditions. The one existing voltage-clamp study of the activation and inactivation kinetics of the sodium current suggests that the voltage and time dependence of the rate coefficients of activation and inactivation in sheep Purkinje fibers at 8°C is similar in form but about an order of magnitude slower than that in the squid giant axon at 15°C. On the basis of comparison of this data with data obtained at 20°C, Dudel and Rudel (1970) predicted that the sodium current should inactivate in less than a millisecond at body temperature. This prediction has since been confirmed by the more recent studies of Ebihara et al. (1980).

Some information about the inactivation process has also been gained by using the

maximum rate of depolarization of the action potential,  $\dot{V}_{\max}$ , as an index of the sodium current. Using a modified voltage-clamp technique, Weidman (1955) showed that the steady-state inactivation curve for  $\dot{V}_{\max}$  has a sigmoidal dependence on membrane potential, similar to the squid giant axon, except that it is steeper by a factor of 1.4. Furthermore, he showed that the time-course of reactivation had a time constant at 37°C varying from 1.4 ms at -106 mV to 10.5 ms at -80 mV.

The aim of our paper is to provide a quantitative description of the kinetics of the sodium carrying mechanism using voltage-clamp data obtained from small spherical clusters of tissue-cultured heart cells. Using the two-microelectrode voltage-clamp technique at 37°C in standard tissue culture medium, Ebihara et al. (1980) demonstrated that in such preparations the kinetics of the fast sodium current could be accounted for equally well by either a coupled or uncoupled kinetic model. We therefore fit our kinetic data to the model of Hodgkin and Huxley (1952) to facilitate the comparison of our kinetics with those of other studies.

## METHODS

The experimental apparatus and protocol, as well as the tissue-cultured spherical cluster of heart cells from which the experimental data used in this paper were obtained, have been described in detail previously (Ebihara et al., 1980). Briefly, the protocol was to record membrane currents during depolarizing voltage-clamp steps from a holding potential of -60 mV. A PDP 11/40 computer (Digital Equipment Corp. Marlboro, Mass.) was used as an on-line data control and data collection system. 700-ms intervals were allowed between depolarizing voltage-clamp steps; all experimental data presented in this paper were obtained at 37°C in standard culture medium. D600-hydrochloride (Knoll, Ludwigshafen an Rhein) (1.25 µg/ml) was used to block time-dependent late currents and to linearize the leakage current in the physiological range (-80 to +20 mV). The data chosen from the study of Ebihara et al. (1980) for quantitative analysis in this paper was not smoothed, nor (because of its brevity) was the initial capacitive transient removed. To take account of the outward rectification of the leakage current at potentials more positive than -20 mV, the traces were fitted to a flat baseline by linear regression analysis and the curves redrawn relative to the fitted baseline. To avoid contamination of the activation phase of the current by the capacitive transient, only points occurring at times later than three time constants of the capacitive transient after its peak were used in the fitting of activation parameters. The data were then fitted to the expression

$$I_{\text{Na}} = \bar{g}_{\text{Na}} m^3 h (V - V_{\text{Na}}), \quad (1)$$

where

$$m(V, t) = m_{\infty}(V) - [m_{\infty}(V) - m_0(V)] \exp [-(t - \Delta t)/\tau_m] \quad (2)$$

and

$$h(V, t) = h_{\infty}(V) - [h_{\infty}(V) - h_0(V)] \exp [-(t - \Delta t)/\tau_h] \quad (3)$$

$$m_{\infty} = \frac{\alpha_m}{\alpha_m + \beta_m} \quad (4a)$$

$$h_{\infty} = \frac{\alpha_h}{\alpha_h + \beta_h} \quad (4b)$$

$$\tau_m = \frac{1}{\alpha_m + \beta_m} \quad (5a)$$

$$\tau_h = \frac{1}{\alpha_h + \beta_h}. \quad (5b)$$

The value of  $m$  at the beginning of the test pulse was set equal to zero and  $h$  was assumed to inactivate fully to zero in the steady state. The initial value for  $h$  was taken from the experimentally determined  $h_\infty$  curve. A delay time,  $\Delta t$ , of 125  $\mu$ s was included in Eqs. 2 and 3 to account for the finite rise time of the voltage-clamp pulse and to provide a better fit to the experimental data.<sup>1</sup>

A nonlinear curve fitting routine, PRAXIS (Brent, 1978), selected values of  $\tau_m$ ,  $\tau_h$ , and  $m_\infty$  to minimize the sum of the squared error of datum minus theory. From these values, the corresponding values for  $\alpha_m$ ,  $\beta_m$ , and  $\beta_h$  were then determined.

### Computer Simulations

Membrane currents in response to step changes in command potential for a membrane patch with and without a series resistance were computed using Eqs. 6–14 to describe the membrane current. The computer program was similar to that published by Palti (1971) for reconstruction of membrane action potentials, except that the membrane current computed at each integration step was applied as a controlling current which caused the recorded membrane potential (sum of the true transmembrane potential and the IR drop across the series resistance) to follow the command potential.

## RESULTS

Noise analysis of the input impedance of preparations similar to those employed in the present studies show the preparation to behave electrically as a lumped, parallel resistance capacitance; none of the membrane capacitance appears to be in series with a resistance or in distributed form, at least in the range of frequencies in our voltage-clamp analyses (Mathias et al., 1980). An effective resistance in series with all the membrane capacitance does appear, however, if the voltage electrode is inserted close to the current electrode, that is, within the three-dimensional electric field about its tip (for discussion of this point, see Ebihara et al., 1980). As was pointed out in that paper, the stability of the voltage-control system was improved when a series resistance of this kind was introduced by approximating the current and voltage electrodes, and such resistance then compensated for by the use of positive current feedback. Analysis of the kinetics of the sodium current was ultimately limited by the speed with which the input capacitance of the preparation could be charged to a new potential. Too much positive current feedback or too little series resistance (the voltage electrode too far from the current electrode) resulted in a ringing (oscillatory) response which partially, if not totally, obscured the activation phase of the sodium current. However, in a few preparations we could reduce the series resistance to small values (<50 k $\Omega$ ) without ringing. Kinetic data from the most completely analyzed preparation are presented here. Similar values for the activation and inactivation time constants were obtained in three other preparations.

### Passive Parameters

The initial capacitive current transient after a step in command potential reached its peak in a time determined by the rise time of the voltage clamp system. As shown in Fig. 1, the fall of the current could be fitted by a single exponential with a time constant of 65  $\mu$ s. The total input resistance, determined by measuring the current associated with a small (–10 mV)

<sup>1</sup>Kootsey, J. M., and E. A. Johnson. 1980. Manuscript submitted for publication.

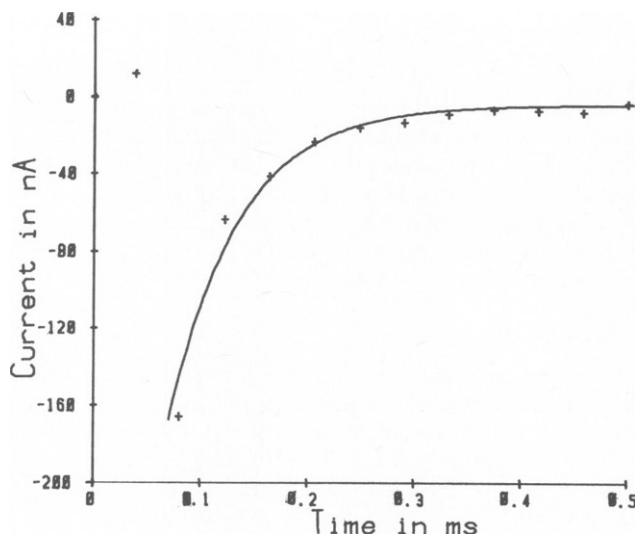


FIGURE 1 Response to a hyperpolarizing potential step to  $-95$  mV. +, experimental results; solid line, exponential fit of the declining phase of the current. Holding potential,  $-60$  mV.

hyperpolarizing step in command potential from a holding potential of  $-60$  mV, was  $2.9$  M $\Omega$ . The input capacitance, estimated by integrating the capacitive transient (extrapolated to zero time), was  $1.2$  nF. The input capacitance was again measured by estimating the membrane area from the diameter and general morphology of the preparation. Electron microscopic studies have shown that  $\sim 15\%$  of the preparation consists of extracellular space and that the average value of the surface area of membrane per unit volume of preparation is  $8,000$  cm $^{-1}$  (footnote 2). Using these values, the observed diameter of  $75$   $\mu$ m, and a specific membrane capacitance of  $1.3$   $\mu$ F/cm $^2$  (Mathias et al., 1980), and neglecting the contribution of nonmuscle cells, we computed, for the preparation from which the chosen data were obtained, a total membrane area of  $1.47 \times 10^{-3}$  cm $^2$  and a corresponding input capacitance of  $1.9$  nF. The series resistance giving the capacitive time constant of  $65$   $\mu$ s for this value of input capacitance is  $34$  k $\Omega$ .

### Sodium Conductance

The form of the functional dependence of the peak value of  $g_{Na}$  on the membrane potential at which it is measured can be determined by plotting the ratio of peak  $I_{Na}/(V - V_{Na})$  against membrane potential, as shown in Fig. 2. These peak values of  $g_{Na}$  are relative to the maximum value obtained at the holding potential of  $-60$  mV. The conductance displays a voltage dependence similar to that observed in other excitable tissues. For small depolarizing steps, it increases  $e$ -fold for a  $4.3$  mV change in potential, leveling off at potentials positive to  $-15$  mV.

A quantitative description of the voltage and time dependency of the current was obtained in the manner first described by Hodgkin and Huxley (1952). The sodium current,  $I_{Na}$ , was

<sup>2</sup>Lieberman, M., and W. Adam. Unpublished data.

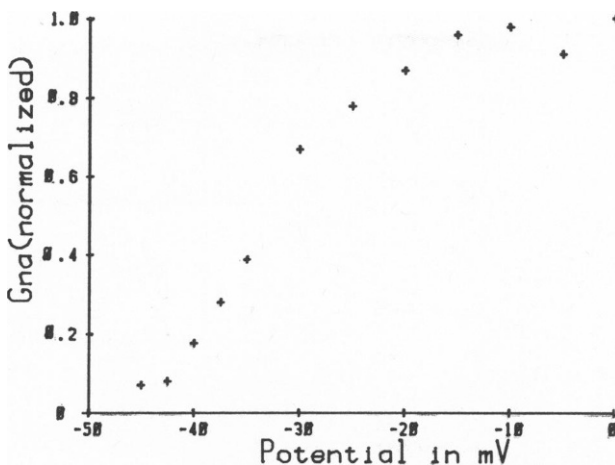


FIGURE 2 Peak sodium conductance normalized with respect to the maximum value obtained. Holding potential,  $-60$  mV.

considered to be given by the following equation:

$$I_{Na} = \bar{g}_{Na} m^3 h (V - V_{Na}), \quad (6)$$

where  $\bar{g}_{Na}$  is a constant (millisiemens),  $V_{Na}$  is the sodium equilibrium potential, and  $m$  and  $h$  are independent, first order, dimensionless variables, which can vary between 0 and 1 as defined by the following differential equations:

$$\frac{dm}{dt} = \alpha_m(1 - m) - \beta_m m \quad (7)$$

$$\frac{dh}{dt} = \alpha_h(1 - h) - \beta_h h, \quad (8)$$

in which  $\alpha_m$ ,  $\alpha_h$ ,  $\beta_m$ , and  $\beta_h$  are instantaneous functions of membrane potential such that solutions of Eqs. 6–8 fit the time-course of the sodium current at a variety of potentials.

The maximum sodium conductance,  $\bar{g}_{Na}$ , was determined in the following way. The steady-state value of  $m$ ,  $m_\infty$ , was set equal to unity over the range of potentials where the peak current was a linear function of potential, i.e., where  $g_{Na}$  was at its maximum and independent of potential. The exponential decay of current at these potentials was extrapolated back to the beginning of the step to give  $\bar{g}_{Na} h_0$ , where  $h_0$  is the initial value of  $h$ .  $h_0$  values were computed from Eqs. 13 and 14 derived below. The value of  $\bar{g}_{Na}$ , determined in this fashion for the preparation chosen for analysis here, was  $23.0 \text{ mS cm}^{-2}$ . Data from two other preparations gave values of 19.5 and  $23 \text{ mS cm}^{-2}$ .

A value of  $+29$  mV was arrived at for  $V_{Na}$  by determining the potential at which the current transient changed in sign. Fig. 3 shows the data used in curve fitting. The dots are data points, whereas the solid lines are solutions of Eqs. 1–3. Table I gives the values of the parameters used in the fitting of the data.

The dependence of  $m_\infty$  and of  $\tau_m$  on membrane potential are shown in Figs. 4 A and B,

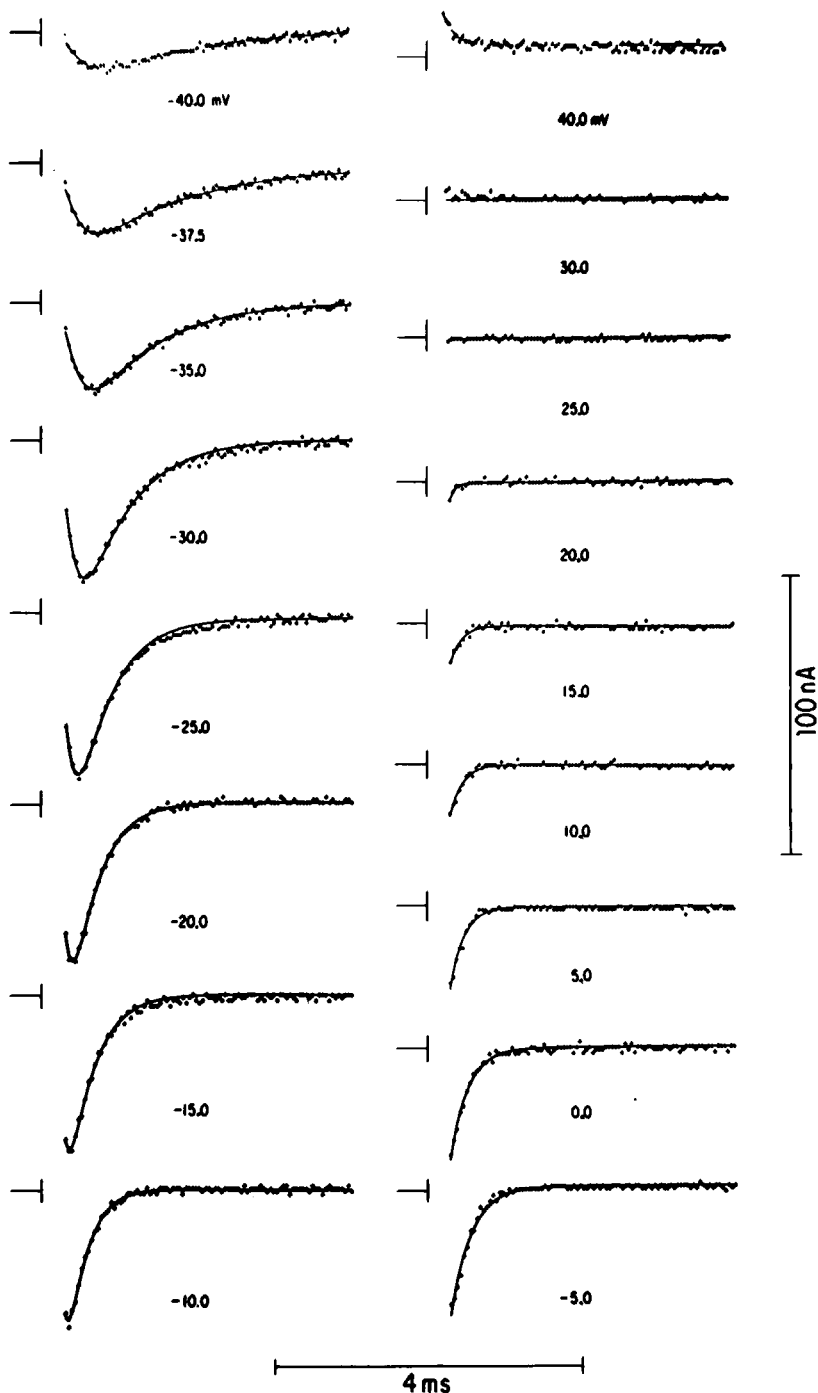


FIGURE 3 Current response to depolarizing steps in command potential. •, experimental points; solid lines, computed from  $I = \bar{g}_{Na} m^3 h (V - V_{Na})$ . Data points occurring earlier than three time constants of the initial capacitive transient after its peak were omitted. Holding potential, -60 mV. Reference bars to left of each trace, zero current and zero time.

TABLE I  
CONSTANTS USED IN  
COMPUTER SIMULATIONS

$C_m$	1.3 $\mu\text{F}/\text{cm}^2$
$\bar{g}_{\text{Na}}$	23.0 $\text{mS}/\text{cm}^2$
$V_{\text{Na}}$	+29.0 mV
$m_0$	0.0
$h_0$	0.18

respectively. Fig. 4 C shows the extrapolated rate coefficients,  $\alpha_m$  and  $\beta_m$ . The solid curves in Fig. 4 C were determined from the following equations:

$$\alpha_m = \frac{0.32 \times (V + 47.13)}{1 - \exp(V + 47.13)} \quad (9)$$

$$\beta_m = 0.08 \times \exp(-V/11), \quad (10)$$

where  $V$  is in millivolts, as were the solid curves in Figs. 4 A and B.

The dependencies of the corresponding parameters for inactivation on membrane potential

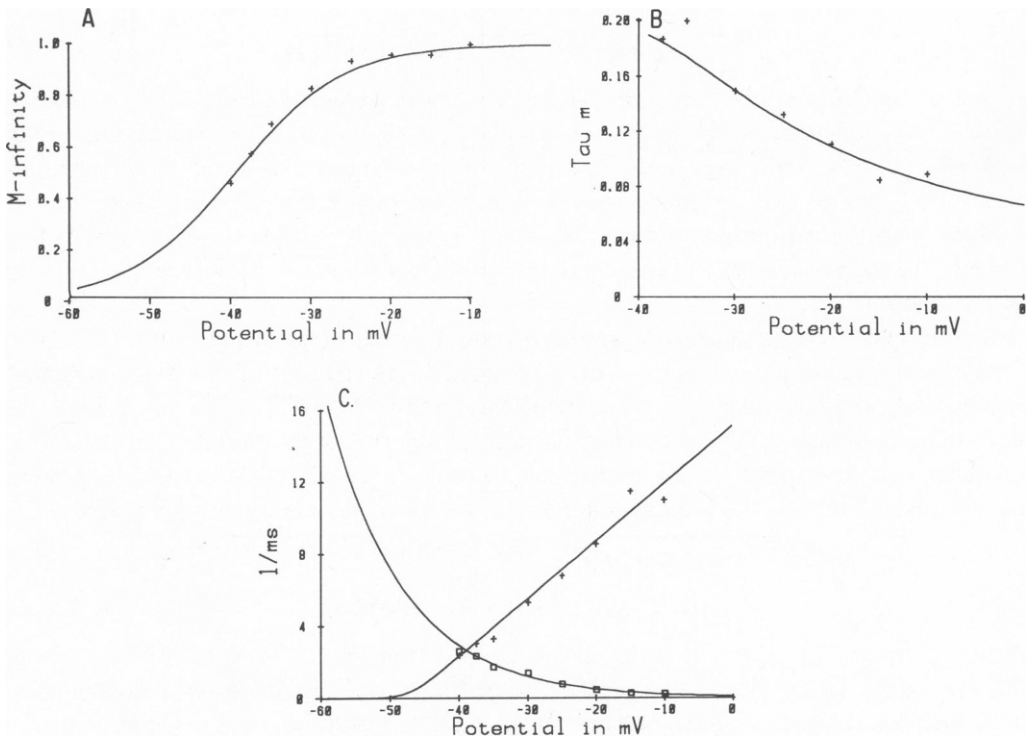


FIGURE 4 (A) Steady-state activation curve. Solid line, computed from Eqs. 9 and 10. (B) Time constant of activation,  $\tau_m$ (ms), as a function of membrane potential. Solid line, computed from Eqs. 9 and 10. (C) Rate coefficients of activation,  $\alpha_m$  (+) and  $\beta_m$  (□) as functions of membrane potential. Solid lines, computed from Eq. 9 ( $\alpha_m$ ) and Eq. 10 ( $\beta_m$ ).

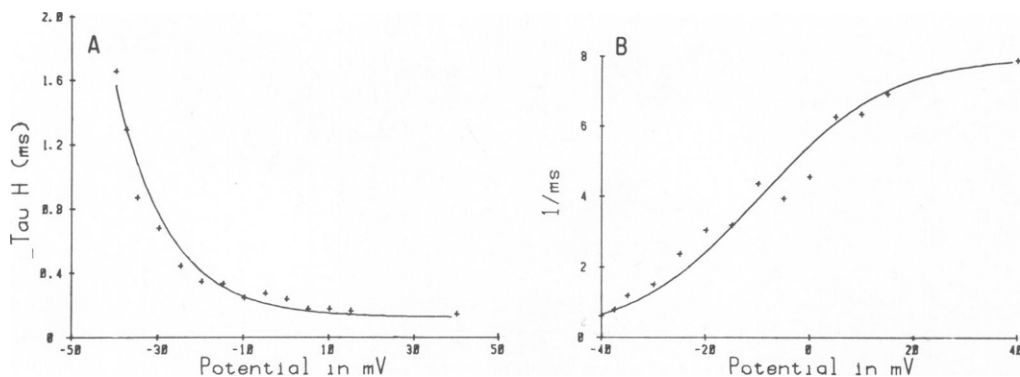


FIGURE 5 (A) Time constant of inactivation,  $\tau_h$ , as a function of membrane potential. Solid line is computed from Eqs. 11 and 12. (B) Rate coefficient of inactivation,  $\beta_h$ , as a function of membrane potential. Solid line, computed from Eq. 12.

are shown in Figs. 5 A and B. The solid curve in Fig. 5 A, for  $V \geq -40$  mV, is described by the equations

$$\alpha_h = 0 \quad (11)$$

$$\beta_h = \frac{1}{0.13 \{ \exp [(V + 10.66)/-11.1] + 1 \}} \quad (12)$$

$\alpha_h$  was set equal to zero for  $V \geq -40$  mV, since previous studies of steady-state inactivation vs. potential (Ebihara et al., 1980) have shown that  $h_\infty$  is zero for potentials more positive than  $-50$  mV. Eq. 12 was also used in the calculation of the solid curves in Fig. 5 B. At potentials positive to  $-10$  mV the sodium current activated too rapidly for the peak current to be resolved from the capacitive transient. However, it was still possible to resolve the falling phase of the sodium current and thereby determine values for  $\tau_h$  for membrane potentials up to  $+40.0$  mV.

No currents were elicited in response to depolarizing steps negative to  $-45$  mV. Consequently, values for  $\alpha_h$  and  $\beta_h$  at these potentials were computed from double potential (conditioning and test) step data over this potential range. Fig. 6 A shows the steady-state inactivation curve as a function of membrane potential for the preparation analyzed here. Fig. 6 B shows the corresponding rate coefficients,  $\alpha_h$  and  $\beta_h$  for potentials equal to and more negative than  $-40$  mV. The solid lines in Fig. 6 C were computed using the expressions,

$$\beta_h = 3.56 \times \exp (0.079 V) + 3.1 \times 10^5 \exp (0.35 V) \quad (13)$$

$$\alpha_h = 0.135 \times \exp [(-80 - V)/6.8]. \quad (14)$$

The solid line in Figs. 6 A and B was also computed from Eqs. 13 and 14. For membrane potentials more positive than  $-45$  mV, the rate coefficient,  $\beta_h$ , determined from double-pulse data, tended to converge with the rate coefficient,  $\beta_h$ , determined from the single-pulse data.

#### Series Resistance

Even though the preparation appears to behave, electrically, as a lumped electrical circuit, indicating that there are no significant variations in transmembrane potential within the



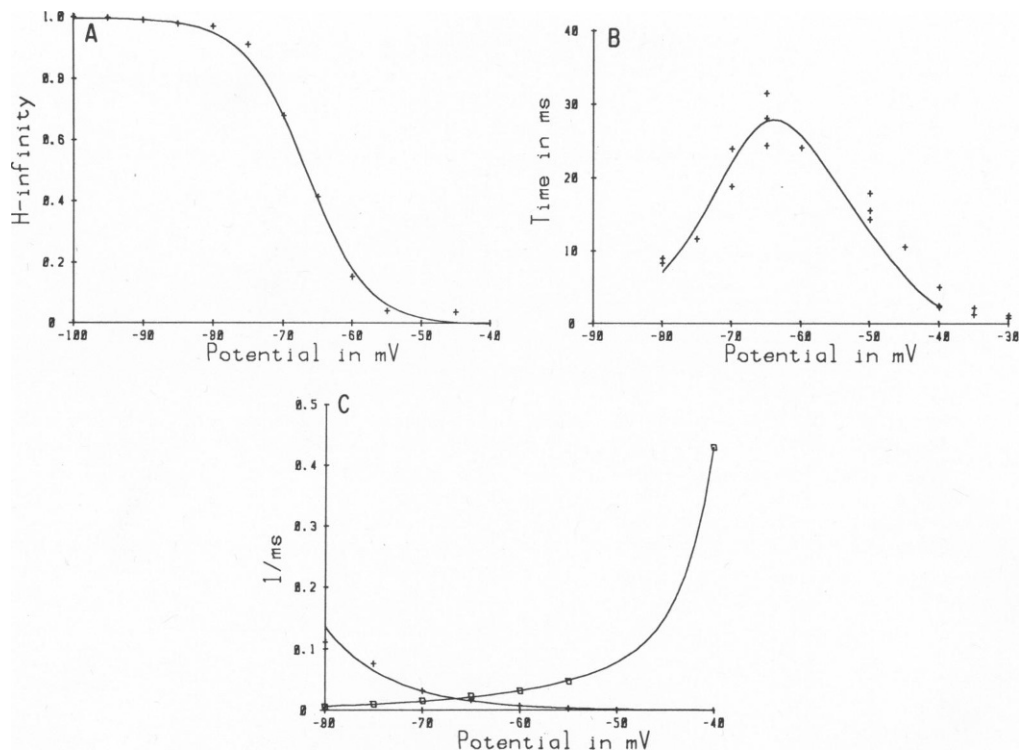


FIGURE 6 (A) Steady-state inactivation curve. Solid line is computed from Eqs. 13 and 14. (B) Time constant of inactivation,  $\tau_h$ , determined from the effects of conditioning prepulses, as a function of membrane potential. Solid line is computed from Eqs. 13 and 14. (C) Rate coefficients of inactivation,  $\alpha_h$  and  $\beta_h$ , determined from the effects of conditioning prepulses. Solid lines are computed from Eq. 13 ( $\alpha_h$ ) and Eq. 14 ( $\beta_h$ ).

preparation, the presence of an effective resistance in series with the membrane can introduce serious errors into voltage-clamp measurements (Bezanilla et al., 1970; Taylor et al., 1966). To better understand and assess the magnitude of the effects of series resistance on our kinetic analysis, we developed a computer simulation of a membrane patch with and without series resistance, using the kinetic parameters that we have computed here for our spherical cluster preparation. These and other parameters of the simulation are given in Table II. Our results show that increasing series resistance caused marked changes in both the shape and magnitude of the inward current transient in response to a depolarizing step to  $-40$  mV. At more positive potentials, the primary effect of series resistance was an initial delay in the onset of the inward current (Fig. 7). The effect of series resistance on the shape and magnitude of the inward transient was minimal for values of series resistance  $< 50$  k $\Omega$ . Thus, there should be no large errors in the data analyzed here, even in the absence of complete series resistance compensation.

As a further test of series resistance, we examined experimentally in the preparation analyzed here the time-course of the sodium current elicited upon depolarization to  $-20$  mV when the magnitude of the current was varied by changing the holding potential. Our results showed that when the peak current magnitude was increased by a factor of 2.4 by changing

TABLE II  
VALUES USED TO COMPUTE RATE COEFFICIENTS

Potential	$m_{\infty}$	$\tau_m$	$h_{\infty}$	$\tau_h$	$\tau_h^*$
(millivolts)		(milliseconds)		(milliseconds)	(milliseconds)
-80	—	—	0.96	—	8.65
-75	—	—	0.88	—	11.6
-70	—	—	0.70	—	21.4
-65	—	—	0.42	—	25.3
-60	—	—	0.19	—	21.3
-55	—	—	0.07	—	20.0
-50	—	—	—	—	13.8
-45	—	—	0.0	—	9.02
-40	0.46	0.20	0.0	1.64	2.36
-37.5	0.58	0.19	—	1.28	1.14
-35.0	0.69	0.2	0.0	0.85	1.14
-30.0	0.83	0.15	0.0	0.66	1.18
-25.0	0.94	0.13	0.0	0.43	—
-20.0	0.96	0.11	0.0	0.33	—
-15.0	0.96	0.09	0.0	0.32	—
-10.0	1.0	0.09	0.0	0.23	—
-5.0	1.0	—	0.0	0.26	—
0.0	1.0	—	0.0	0.22	—
5.0	1.0	—	0.0	0.16	—
10.0	1.0	—	0.0	0.16	—
15.0	1.0	—	0.0	0.15	—
40.0	1.0	—	0.0	0.13	—

\*Time constant of inactivation determined by a double pulse method.

the holding potential from  $-60$  to  $-65$  mV, no change in time to peak or time constant of inactivation was observed.

## DISCUSSION

Models of the generation of the cardiac action potential (McAllister et al., 1975; Beeler and Reuter, 1977) have had to include *ad hoc* assumptions as to the kinetics of the sodium channel, because until recently there has been no firm experimental evidence on which to base

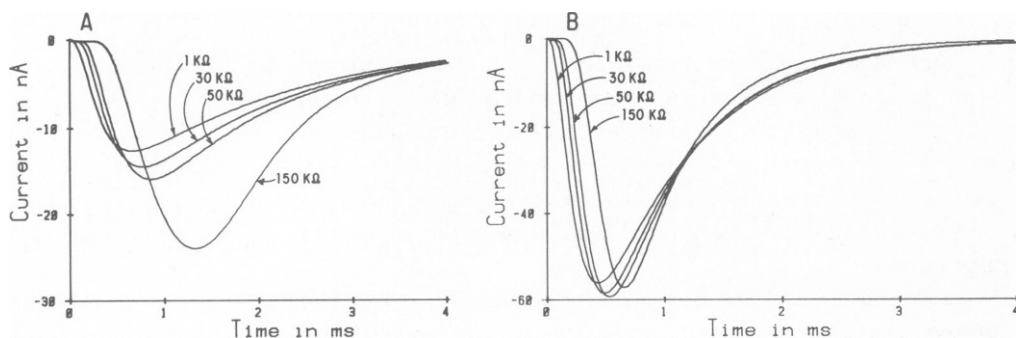


FIGURE 7 Effect of series resistance on the time-course of the inward current computed as described in the text. (A)  $-40$  mV, (B)  $-20$  mV.

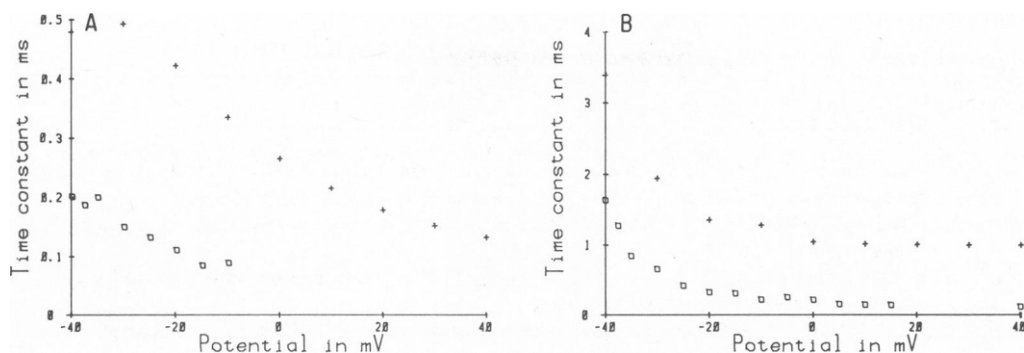


FIGURE 8 Comparison of time constants  $\tau_m$  (A) and  $\tau_h$  (B) as a function of membrane potential for (+) squid axon at 15°C (Hodgkin and Huxley, 1952) and (□) cardiac muscle (cultured cluster) at 37°C.

such assumptions. Although the starting point of all the models has been the Hodgkin-Huxley equations, the characteristics of the sodium channel were greatly modified when kinetic parameters were manipulated to agree with what little experimental evidence was available. For example, the ratio of inactivation to activation time constants,  $\tau_h/\tau_m$ , in the range  $-40$ – $0$  mv, is 3–5 for the squid, whereas it is 32–63 in the model of Beeler and Reuter (1977) for mammalian ventricular muscle, and 28–104 in the model of McAllister et al. (1975) for ungulate Purkinje fibers. Moreover, the maximum sodium conductance,  $\bar{g}_{Na}$ , is  $120 \text{ mS cm}^{-2}$  in the squid axon, whereas in the model of Beeler and Reuter it is  $4 \text{ mS cm}^{-2}$ .

In our kinetic description of the fast sodium current presented here, the ratio,  $\tau_h/\tau_m$ , is similar to that of the squid axon, varying from 8 at  $-40$  mV to 2.6 at  $-10$  mV. Moreover, the dependency on potential of the observed and theoretical values of the time constants,  $\tau_m$  and  $\tau_h$ , at 37°C, is similar to that of the squid at 15°C, except that the magnitude of the time constants for the squid are slower than for the heart, as evident from Fig. 8. As in the model of Beeler and Reuter (1975), we found  $\bar{g}_{Na}$  to be considerably smaller than that of squid. Furthermore, our curve for steady-state inactivation as a function of potential is shifted  $\sim 12$  mV in the hyperpolarizing direction as compared with that of squid. Consequently, there is almost no overlap between the  $m_\infty$  and  $h_\infty$  curves, with the sodium current inactivating completely at all potentials. Similar findings were reported by Colatsky and Tsien (1979) in rabbit Purkinje strands and by Dudel and Rudel (1970) for sheep Purkinje strands. Weidman's results (1955) also suggest that  $h_\infty$  is very small at potentials positive to  $-40$  mV. This result differs from the findings of Gadsby and Cranfield (1977) and Attwell et al., (1979) which predict a steady-state TTX-sensitive ("window") sodium current in cardiac Purkinje fibers.

The quantitative analysis presented here is consistent with the statement of Ebihara et al. (1980) that cardiac muscle and the squid giant axon share the same kind of permeability mechanism. We should point out, however, that the time resolution of the activation data is insufficient to show the necessity for  $m^3$  kinetics.

We would like to express special thanks and appreciation to Doctors Lieberman and Shigeto, our colleagues in the experimental work on which this paper is based. We also wish to express our thanks to Mailen Kootsey and Dennis Rockwell for advise and assistance in the computations and to Pat Purcell for her word processing.

The work was supported by National Institutes of Health grant 2-P01-HL-12157.

Received for publication 21 March 1980 and in revised form 7 July 1980.

## REFERENCES

- ATTWELL, D., I. COHEN, D. EISNER, M. OHBA, and C. OJEDA. 1979. The steady-state TTX-sensitive ("window") sodium current in cardiac Purkinje fibres. *Pfluegers Arch. Eur. J. Physiol.* 379:137-142.
- BEELER, G. W., and H. REUTER. 1977. Reconstruction of the action potential of ventricular myocardial fibres. *J. Physiol. (Lond.)* 268:177-210.
- BEZANILLA, F., E. ROJAS, and R. E. TAYLOR. 1970. Sodium and potassium conductance changes during a membrane action potential. *J. Physiol. (Lond.)* 211:729-751.
- BRENT, R. P. 1978. Algorithms for Minimization Without Derivation. Prentice-Hall, Inc., Englewood Cliffs, N.J. 185.
- COLATSKY T. J., and R. W. TSIEN. 1979. Sodium channels in rabbit cardiac Purkinje fibers. *Nature (Lond.)* 278:265-268.
- DUDEL, J., and R. RUDEL. 1970. Voltage and time dependence of excitatory sodium current in cooled sheep Purkinje fibres. *Pfluegers Archiv. Gesamte Physiol. Menschen Tiere* 315:136-158.
- EBIHARA, L., N. SHIGETO, M. LIEBERMAN, and E. A. JOHNSON. 1980. The initial inward current in spherical clusters of chick embryonic heart cells. *J. Gen. Physiol.* 75:437-456.
- GADSBY, D. C., and P. CRANFIELD. 1977. Two levels of resting potential in cardiac Purkinje fibers. *J. Gen. Physiol.* 70:725-746.
- HODGKIN, A. L., and A. F. HUXLEY. 1952. A quantitative description of membrane current and its application to conduction and excitation in nerve. *J. Physiol. (Lond.)* 117:500-544.
- JOHNSON, E. A., and M. LIEBERMAN. 1971. Heart: excitation and contraction. *Annu. Rev. Physiol.* 33:479-532.
- MATHIAS, R. T., L. EBIHARA, M. LIEBERMAN, and E. A. JOHNSON. 1980. Analysis of the linear electrical properties of cultured clusters of embryonic chick heart cells. *Fed. Proc. (Abstr.)*.
- MCALLISTER, R. E., D. NOBLE, and R. W. TSIEN. 1975. Reconstruction of the electrical activity of cardiac Purkinje fibres. *J. Physiol. (Lond.)* 251:1-59.
- PALTI, Y. 1971. Description of axon membrane ionic conductances and currents. In *Biophysics and Physiology of Excitable Membranes*. W. J. Adelman, Jr., editor. Van Nostrand Reinhold Co, New York.
- REUTER, H. 1979. Properties of two inward membrane currents in the heart. *Annu. Rev. Physiol.* 41:413-424.
- TAYLOR, R. E., J. W. MOORE, and K. S. COLE. 1966. Analysis of certain errors in squid axon voltage clamp measurements. *Biophys. J.* 1:161-202.
- WEIDMAN, S. 1955. The effect of the cardiac membrane potential on the rapid availability of the sodium carrying system. *J. Physiol. (Lond.)* 127:213-224.